Frontiers in Bioscience Landmark

Front. Biosci. (Landmark Ed) **2023**; 28(12): 325
https://doi.org/10.31083/j.fbl2812325

Original Research

Maintenance of the Expression of c-FLIP$_L$ by Hsp70 to Resist Licochalcone A-Induced Anti-Colorectal Cancer Effect through ERK-Mediated Autophagy Induction

Tianpeng Li[1,†], Ting Li[1,†], Hongbin Zhang[2], Chunyan Liu[3], Min Li[4], Chu Wang[4], Yuanyuan Zheng[4], Lihua Zhang[5], Xiaoyi Long[6], Shaoqing Shi[7], Yun Long[8,*], Wei Chen[1,*]

[1]Institute of Basic Medicine and Forensic Medicine, Medical Imaging Key Laboratory of Sichuan Province, North Sichuan Medical College, 637000 Nanchong, Sichuan, China
[2]Department of Pediatric Surgery, the First Affiliated Hospital of Kunming Medical University, 650032 Kunming, Yunnan, China
[3]Institute of School Health, Yunnan Center for Disease Control and Prevention, 650032 Kunming, Yunnan, China
[4]Department of Respiratory Medicine, the First Affiliated Hospital of Kunming Medical University, 650032 Kunming, Yunnan, China
[5]Department of General Medicine, the First Affiliated Hospital of Kunming Medical University, 650032 Kunming, Yunnan, China
[6]Department of Pathophysiology, Institute of Basic Medicine and Forensic Medicine, North Sichuan Medical College, 637000 Nanchong, Sichuan, China
[7]Scientific Research Laboratory Center, the First Affiliated Hospital of Kunming Medical University, 650032 Kunming, Yunnan, China
[8]Department of General Medicine, Kunming Yan'an Hospital, 650051 Kunming, Yunnan, China
*Correspondence: longyun0514@126.com (Yun Long); chengwei197959@163.com (Wei Chen)
[†]These authors contributed equally.

Academic Editor: Fu Wang
Submitted: 17 April 2023 Revised: 4 June 2023 Accepted: 9 June 2023 Published: 1 December 2023

Abstract

Background: The mortality rate of colorectal cancer (CRC) ranks second worldwide. Previous research had indicated that licochalcone A (LA) was a flavonoid in licorice with diverse anticancer effects. We explored the underlying mechanisms of LA-triggered anticancer activity in CRC. **Methods**: Thiazolyl Blue (MTT) experiment and EdU staining were utilized to evaluate cell proliferation. Meanwhile, cells were stained by Annexin V/PI to investigate apoptosis through flow cytometry assay. Moreover, expressions of proteins were detected by immunoblotting, and the level of related mRNA was investigated using real-time quantitative PCR. **Results**: LA selectively suppressed the proliferation and triggered apoptosis of CRC cells. Strikingly, LA induced cytoprotective autophagic activities since the suppression of autophagy significantly strengthened LA-induced cytotoxicity and FLICE inhibitory protein (c-FLIP$_L$) degradation, meanwhile reversing LA-mediated heat shock protein 70 (Hsp70) upregulation. Moreover, autophagy-mediated Hsp70 upregulation resisted LA-induced anticancer effects since the suppression of Hsp70 strengthened LA-triggered cytotoxicity and c-FLIP$_L$ degradation. Furthermore, LA greatly activated extracellular signal-regulated protein kinases (ERK) and p38. However, blocking of ERK, but not p38, significantly boosted LA-triggered cell death and c-FLIP$_L$ downregulation. Suppression of ERK also reversed LA-mediated autophagic induction. **Conclusions**: LA increased Hsp70 expression depending on ERK-mediated autophagy, which protected CRC cells from LA-induced anticancer activities.

Keywords: colorectal cancer; licochalcone A; Hsp70; ERK; apoptosis; autophagy

1. Introduction

According to global cancer data for 2020, colorectal cancer (CRC) had the second-highest mortality rate and accounted for approximately 9% of all cancer-related deaths each year worldwide [1]. It was reported that the incidence of CRC worldwide was expected to rise to about 2.5 million in developing countries until 2035 [2]. Diagnosing CRC is difficult because its symptoms appear only at a late stage, and its mechanisms are elusive. The five-year relative survival rate in low-income countries remained below 50% [3–5]. The drug resistance of anticancer drugs is becoming gradually serious because of the complexity of the tumorigenesis mechanism. The search for novel anticancer drugs with superior anticancer effects and novel mechanisms has become one of the key targets for researchers.

In recent years, the powerful anticancer effects and low side effects of herbal extracts have attracted the attention of medical researchers worldwide. Our previous studies have demonstrated that Chalcones were a promising class of anticancer agents [6–9]. Licochalcone A (LA) is a chalcone in licorice with effective antitumor activities [10–15], and the poor bioavailability of LA was solved by loading on liposome carriers [16]. It was reported that LA induced autophagy by activating mitogen-activated protein kinase (MAPKs), including extracellular signal-regulated protein kinases (ERK), p38, and c-Jun N-terminal kinase (JNK), in lung cancer [9,17–19]. However, the effects and mechanisms of MAPKs and autophagy in LA-induced anti-CRC activities remain elusive.

During our research, we found that autophagy could maintain the expression of FLICE inhibitory protein (c-$FLIP_L$), an important apoptosis suppressor protein. As reported, heat shock proteins (HSPs), including heat shock protein 70 (Hsp70) and heat shock protein 90 (Hsp90), could maintain the expression of c-$FLIP_L$ in lung cancer [20,21]. Heat shock proteins (HSPs) assist the maturation of diverse proteins, including those that play a crucial part in cancer development [22,23]. Therefore, the roles of autophagy, c-$FLIP_L$, and HSPs were explored in anticancer activities induced by LA.

In our research, LA was found to restrain cell viability and trigger cell apoptosis in CRC cells. However, LA triggered cytoprotective autophagy in CRC cells. This autophagy enhanced Hsp70 expression, maintaining the expression of its downstream c-$FLIP_L$, which reduced cell apoptosis. Subsequently, we explored the mechanisms of MAPKs in LA-triggered autophagic induction in CRC cells. Consequently, LA was found to trigger autophagic induction through activation of ERK signaling pathways, which in turn inhibited apoptosis. Conclusively, LA increased Hsp70 expression depending on ERK-mediated autophagy induction, which maintained the expression of c-$FLIP_L$, resulting in CRC cell resistance to LA *in vitro*. Therefore, our results provided novel evidence for the mechanism of CRC cell resistance to LA, and it is necessary to further explore the mechanism of LA in the treatment of CRC.

2. Materials and Methods

2.1 Reagents and Antibodies

Antibodies for phosphor-p38 MAPK (4511), PARP (9542), and LC3 (4108) were from Cell Signaling Technology (Boston, Massachusetts, USA). Antibody for HSPA4 (381501), JNK1 (201001), P44/42 MAPK (ERK1/2) (250222), p38 (220979), Hsp90 alpha (209902), GAPDH (200306-7E4), β-tubulin (200608) were from Zen Bioscience (Chengdu, China). Anti-caspase 3 (ab32351) and c-$FLIP_L$ (ab8421) were from Abcam (Cambridge, UK). Anti-phospho-JNK (2679369) and phosphor-MAP kinase 1/2 (ERK1/2) were from Millipore (Boston, MA, USA). Licochalcone A (HY-N0372), U0126 (HY-12031A), SB203580 (HY-10256), MKT-077 (HY-15096), z-VAD-fmk (HY-16658B), Chloroquine (CQ) (HY-17589A) and Thiazolyl Blue (HY-15924) were from MCE MedChemExpress (Monmouth Junction, New Jersey, USA).

2.2 Cell Culture

NCM460 of normal human colonic epithelial and HT29 cell line was from JENNIO Biological Technology (China). Colon cancer cell lines SW620 and HCT116 were purchased from Procell Life Science & Technology Co., Ltd. (China). NCM460 grew in RPIM 1640 mediums. SW620 cells grew in DMEM mediums. HT29 and HCT116 cells grew in MCCOY'S 5A mediums. These mediums were added with fetal bovine serum (FBS) (1:10), L-glutamine (2 mmol/L), penicillin (100 U/mL), and streptomycin (100 µg/mL). All cells were held at 37 °C with 5% CO_2 and were mycoplasma-free (Yeasen Mycoplasma Detection Kit). MCCOY'S 5A mediums without fetal bovine serum were from Solarbio (Beijing, China). RPIM 1640 medium and DMEM medium without FBS were obtained from Gibco (Grand Island, New York, USA). All cell lines were authenticated shortly before use by the STR technique, carried out by manufacturers.

2.3 Cell Viability Assay

Thiazolyl Blue (MTT) experiment was used to investigate the cytotoxic activities of LA. CRC cells were divided into three parts and plated in 48-well plates (2.5×10^4/well) and overnight, next cultured with MTT (20 mg/mL) at 37 °C. After 3 h, mediums were discarded, and MTT crystals were treated with 100 µL DMSO for 10 min. Next, the optical densities were measured using a fluorescent plate reader (Olympus CKX41, Tokyo, Japan) at OD_{570}. Then, the inhibitory rates of cell growth were computed as follows: (A control - A treated)/A control $\times$ 100%, where A treated and A control is the absorbance of the treated and control groups, respectively. Each experiment was performed in quadruplicate and repeated at least three times.

2.4 Colony Forming

The proliferation effects of LA on SW620 cells were investigated with a colony formation experiment. CRC cell line was grown in six-well plates (2×10^4 cells/well). Then, they were incubated with diverse thicknesses of LA. After 7 days (change the mediums with LA every 3 days), mediums were discarded, and cells were treated with paraformaldehyde for 15 min. Then, Colony formation was photographed after being treated using 0.1% crystal violet dye for 10 min.

2.5 EdU Staining

CRC cell line gown in 48-well plates, next, exposed to DMSO (0.1%) or LA for 8 h at 37 °C. Then, discarded the old culture medium from the 48-well plates and added 200 µL medium containing LA and EdU (medium: EdU solution = 1000:1) to each well for 2 h. Cells were treated with 2 mg/mL glycine and 0.5% TritonX-100 after being fixed with 4% paraformaldehyde. Next, DNA syntheses were measured by the EdU Apollo488 Imaging Kit according to recommendations (RiboBio, Guangzhou, China).

2.6 Immunofluorescence Staining

Cells were grown in 48-well plates and, next, cultured with CQ, U0126, and LA for 8 h at 37 °C. Then, cells were treated with Methanol precooled at –20 °C and were exposed to Triton X-100 diluted in PBST (1:200) at 20 °C. After 30 min, they were treated with BSA (1:20 diluted in PBST) for 1 h and held at 4 °C for 12 h with an antibody

Table 1. Primer sequences for RT-PCR.

Genes name	5′-3′ primer	3′-5′ primer
c-FLIP$_L$	GCAGTCTCACAGCTCACCAT	GTGCTGCAGCCAGACATAA
Hsp70	GAAGCCTGTAGTTGACTGTGTTGTTTC	AATCGCAAGCAATTAAGACCAGCAATC
Hsp90	AACCCTGACCATTCCATTATTGAGACC	GCAAGATGACCAGATCCTTCACAGAC

against LC3 (1:200 diluted in PBST). Then, cells were held with an anti-rabbit antibody which was conjugated to Alexa Fluor 594. After 1 h, DAPI was used to stain the nucleus for 5 min, and cells were examined with a fluorescence microscope instrument (Olympus CKX41, Japan) immediately.

2.7 Cell Cycle

CRC cell lines were grown in 6-well plates (6×10^6 cells/well) and, 12 h later, were grown with LA. After 8 h, the collected cells were fixed with ethanol (70%) for 12 h at –20 °C. After that, cells were treated with propidium iodides (PI) for 30 min. Quantitation of the cell cycle ratio was measured by an Accuri C6 flow cytometry instrument (BD Biosciences, Franklin Lakes, New Jersey, USA).

2.8 Annexin V-FITC/PI Double-Stained Assays

Apoptotic cell death of CRC was measured by Annexin V-FITC Apoptosis Detection Kit (BD Biosciences). CRC cell line grown in 6-well plates. Then, they were grown with DMSO (0.1%) or 20 µM LA. After 48 h, cells were harvested after being treated with 0.25% Trypsin. Next, the binding buffer with PI (5 µL) and Annexin V (FITC-conjugated) (5 µL) was used to treat cells for 15 min in the dark at room temperature. After that, the Accuri C6 flow cytometry instrument (BD Biosciences) was utilized to detect cell apoptosis. The percentages of AnnexinV-FITC/7AAD stained cells were analyzed by Flowjo 10.0 software (Tree Star, San Carlos, California, USA). Experiments were repeated at least three times, and representative results are shown in each figure.

2.9 RNA Extraction and Real-Time Quantitative RT-PCR

All RNA was separated from CRC cells by Trizol (Ambion, Waltham, Massachusetts, USA). The process of quantification includes two reactions. The first reaction is reverse transcription which used FastKing RT Kit (gDNase) (TIANGEN, Beijing, China) in a reaction system of 20 µL. Reactions were carried out in a C1000 TouchTM Thermal Cycler (BIO-RAD, Hercules, California, USA) at 42 °C for 15 min, then heat inactivation at 95 °C for 3 min. After that, the reverse transcription reaction system was mixed with water without nuclease and held at –80 °C.

The second reaction is Real-time PCR which was carried out using rotorgene Q 2plex HRM (QIAGEN, Hilden, Germany) with SuperReal PreMix Plus (SYBR Green) (TIANGEN) with a 20 µL PCR reaction system. Each sample was divided into three parts to run and analyze. After the PCR cycle reaction, an analysis of the melting curve was carried out to prove the specificity of PCR products. In addition, primer sequences of c-FLIP$_L$, Hsp70, and Hsp90 were designed and synthesized by Sangon Biotech (Table 1).

2.10 Western Blot

Radio immunoprecipitation assay buffer was used to lyse cells. Then, whole cell lysates were centrifugated, and the supernatant fraction was collected for immunoblotting. Protein concentrations of supernatant fraction were investigated by the bicinchoninic acid (BCA) experiment. Then, proteins were incubated at 100 °C for 10 min. After that, equal proteins were extracted from the lytic sample, then distributed by SDS-PAGE. Afterward, protein molecules were metastasized to polyvinylidene difluoride membrane in an electric field. After that, it was exposed to tris buffered saline with Tween-20 (TBST), including non-fat milk powder (1:20). After 2 h; the membrane was exposed to primary antibodies with specificity at 4 °C for 12 h. The next day, it was exposed to secondary antibodies (horseradish peroxidase-conjugated). Immunoreactivities were investigated by the enhanced chemiluminescence (ECL) system (Millipore). Each experiment was carried out 3 times; then representative consequences were shown.

2.11 Cycloheximide Chasing Assay

CRC cell lines were grown in 12-well plates (3×10^6 cells/well) and, 12 h later, were incubated with LA or DMSO for 8 h. Next; cells were treated with CHX (200 µg/mL). Radio immunoprecipitation assay buffer was used to lyse cells at 0, 0.5, 1, 2, and 4 h. Then, whole cell lysates were centrifugated, and the supernatant fraction was collected for immunoblotting.

2.12 Statistical Analysis

All statistics were shown as mean ± SD and were assessed using SPSS 25.0 for Windows (SPSS Inc., Armonk, New York, USA). The differences between the two groups were determined using two-tailed *t*-tests. The differences among three or more groups were determined using one-way analysis of variance (ANOVA). $p < 0.05$ was viewed as statistically significant.

3. Results

3.1 LA Caused Cell Growth Inhibition and Arrested Cell Cycle in CRC

To interrogate the anticancer effects of LA in CRC *in vitro*, SW620, HCT116, HT29, and normal colonic epithe-

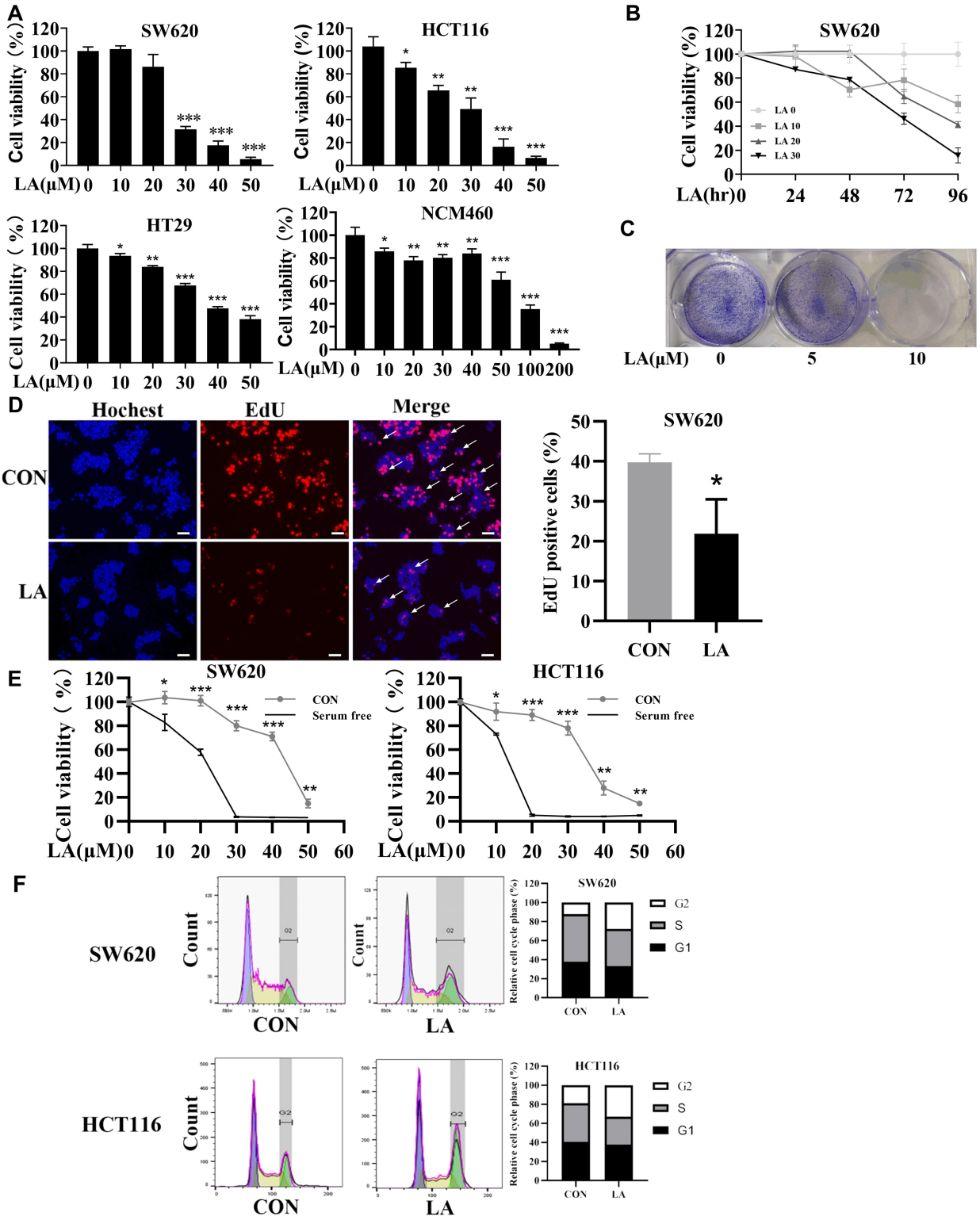

Fig. 1. The suppression of licochalcone A (LA) on colorectal cancer (CRC) cell proliferation is significantly greater than its toxicity to normal cells. (A) different thickness of LA was used to treat SW620, HCT116, HT29 and NCM460 cells. After 48 h, cell proliferations were detected by Thiazolyl Blue (MTT) experiment. (B) SW620 cells were cultured with diverse thickness LA, and then cell viability was tested by MTT experiment at 24, 48, 72, and 96 h. (C) SW620 cells were cultured with LA (0, 5, and 10 μM) for 7 days; then crystal violet staining was carried out. (D) SW620 cells were cultured with 20 μM LA for 8 h; next, EdU staining was performed. Scale bar 100 μm. (E) SW620 and HCT116 were cultured with LA (0, 10, 20, 30, 40, and 50 μM) for 48 h in cultures with serum or not, and then cell viabilities were measured by MTT experiment. (F) SW620 and HCT116 cells were cultured with LA (20 μM); next, flow cytometric assay was utilized to examine the cell cycle at 8 h. N = 3. *$p < 0.05$, **$p < 0.01$, ***$p < 0.001$.

lial cell line NCM460 grown with diverse thicknesses of LA for 48 h, and next cell viabilities were investigated by MTT experiment. Then, LA was proved to suppress the viability of CRC cells (Fig. 1A). The 50% inhibition concentrations (IC50) for 48 h of LA treatment were 26.4 μM, 30.6 μM, 41.5 μM, and 89.4 μM for the SW620, HCT116, HT29, and NCM460 cells respectively, indicating that LA selectively inhibited CRC cells. It seems that KRAS-mutated CRC cells (SW620 and HCT116) were more sensitive to LA compared with KRAS wild HT29 cells. Similarly, SW620 cells were exposed to diverse thicknesses of LA, then the cell viabilities were detected by MTT experiment at 24, 48, 72, and 96 h (Fig. 1B). Then, LA was proved attenuated the viabilities of CRC cells dose- and time-dependently. Consistently, colony formation assay demonstrated that LA inhibited single CRC cells proliferation (Fig. 1C), and EdU staining showed that LA inhibited DNA synthesis of CRC cells (Fig. 1D). Moreover, LA-induced cell viability inhibition was significantly enhanced under starvation stimulation, indicating that LA might effectively inhibit CRC cells under stress conditions (Fig. 1E).

To further investigate the effects of LA in CRC, we detected the cell cycle under LA-induced anticancer activity of SW620 and HCT116 cells. Flow cytometry analysis discovered that significant increase (from 12.1% to 26.5% in SW620 cells and from 18.9% to 33.1% in HCT116 cells) in the ratio of G2 phase in cells after being treated with LA, indicating that the CRC cells cycle was arrest in G2/M phase by LA (Fig. 1F). In summary, LA selectively suppressed CRC cells by inducing arrest in G2/M cell cycle.

3.2 LA Triggered Apoptosis in CRC Cells

Next, we investigated the relationship of apoptosis in LA-triggered cell death by Annexin V/PI experiment. Flow cytometric results indicated that LA enhanced apoptosis of CRC cells (Fig. 2A). Meanwhile, LA greatly augmented the level of hallmark proteins of apoptosis (cleaved caspase-3 and PARP) (Fig. 2B). Furthermore, pan-caspase inhibitor (z-VAD-fmk) greatly compromised LA-triggered cytotoxicity (Fig. 2C), further supporting that LA induced cell apoptosis of CRC.

Recently, there was growing evidence that c-FLIP$_L$ could be used as a target to repair the apoptotic reaction of cancer cells [24]. Therefore, we examined the level of c-FLIP$_L$ in CRC cells. Then, LA was discovered inhibited c-FLIP$_L$ expression (Fig. 2D) rather than its mRNA level (Fig. 2E) in SW620 cells. Furthermore, the cycloheximide chasing assay suggested that LA did not accelerate the degradation of c-FLIP$_L$ (Fig. 2F). This indicated that the inhibition of c-FLIP$_L$ by LA was independent of transcription and degradation and might be related to the translation of its mRNA. Collectively, LA induced cell apoptosis of CRC.

3.3 ERK Activation Resisted LA-Induced Cytotoxicity in CRC

MAPKs are associated with LA-triggered anticancer effects. However, the roles of MAPKs are elusive in CRC. Thereby, we explored mechanisms of MAPKs in LA-induced anticancer activity. Then, LA was found indeed to activate ERK and p38 time-dependently in SW620 and HCT116 cells. Whereas the impact of LA on JNK activity was not obvious in SW620 and HCT116 cells (Fig. 3A). After that, we interrogated the role of ERK and p38 in LA-triggered anticancer activity. The results discovered that ERK inhibitor U0126, not p38 inhibitor SB203580, remarkably promoted LA-induced inhibition of SW620 cell viability (Fig. 3B), indicating that ERK activation resisted LA-triggered anticancer activities in SW620 cells, not HCT116 cells. Therefore, we explored the role of ERK in the LA-induced apoptosis of SW620 cells. The results showed that U0126 enhanced cell apoptosis (Fig. 3C), augmented cl-caspase-3 and cl-PARP expression, and further promoted the downregulation of c-FLIP$_L$ in LA-induced anti-CRC activity (Fig. 3D). This indicated that the activation of ERK resisted LA-induced cytotoxicity in SW620 cells.

3.4 LA Triggered Protective Autophagy by ERK Activation in CRC Cells

Previous studies have demonstrated LA induced autophagy in diverse types of cancers [13–15,17,19]. Whereas mechanisms about autophagy in LA-triggered anticancer activity were controversial. Therefore, we investigated mechanisms of autophagic induction in LA-triggered anti-CRC effects. Then, LA was discovered to induce LC3-II accumulation (Fig. 4A), indicating LA might increase autophagic activities in SW620 cells. These results were further supported by the autophagic flux assay (Fig. 4B). Consistently, immunofluorescence staining also discovered that CQ blocked LA-induced autophagic flux (Fig. 4C). To uncover the role of autophagic induction in LA-triggered anticancer effects, CQ was used to block the activity of autophagy. As shown in Fig. 4D and 4E, CQ significantly augmented LA-triggered apoptosis of CRC cells and enhanced the level of cl-caspase-3 and cl-PARP, meanwhile downregulated the level of c-FLIP$_L$ (Fig. 4F). Which discovered that autophagic induction played a protective role by maintained c-FLIP$_L$ expression in LA-triggered cytotoxicity.

Thereby, we explored the relationship between ERK and autophagy in LA-triggered anticancer effects. The Western blot (Fig. 4G) and immunofluorescence staining (Fig. 4H) results showed that U0126 suppressed LA-induced LC3-II accumulation in SW620 cells, which indicated that LA triggered autophagic induction by ERK activation. Therefore, autophagy activation mediated by ERK played a protective part in LA-triggered anti-CRC effects.

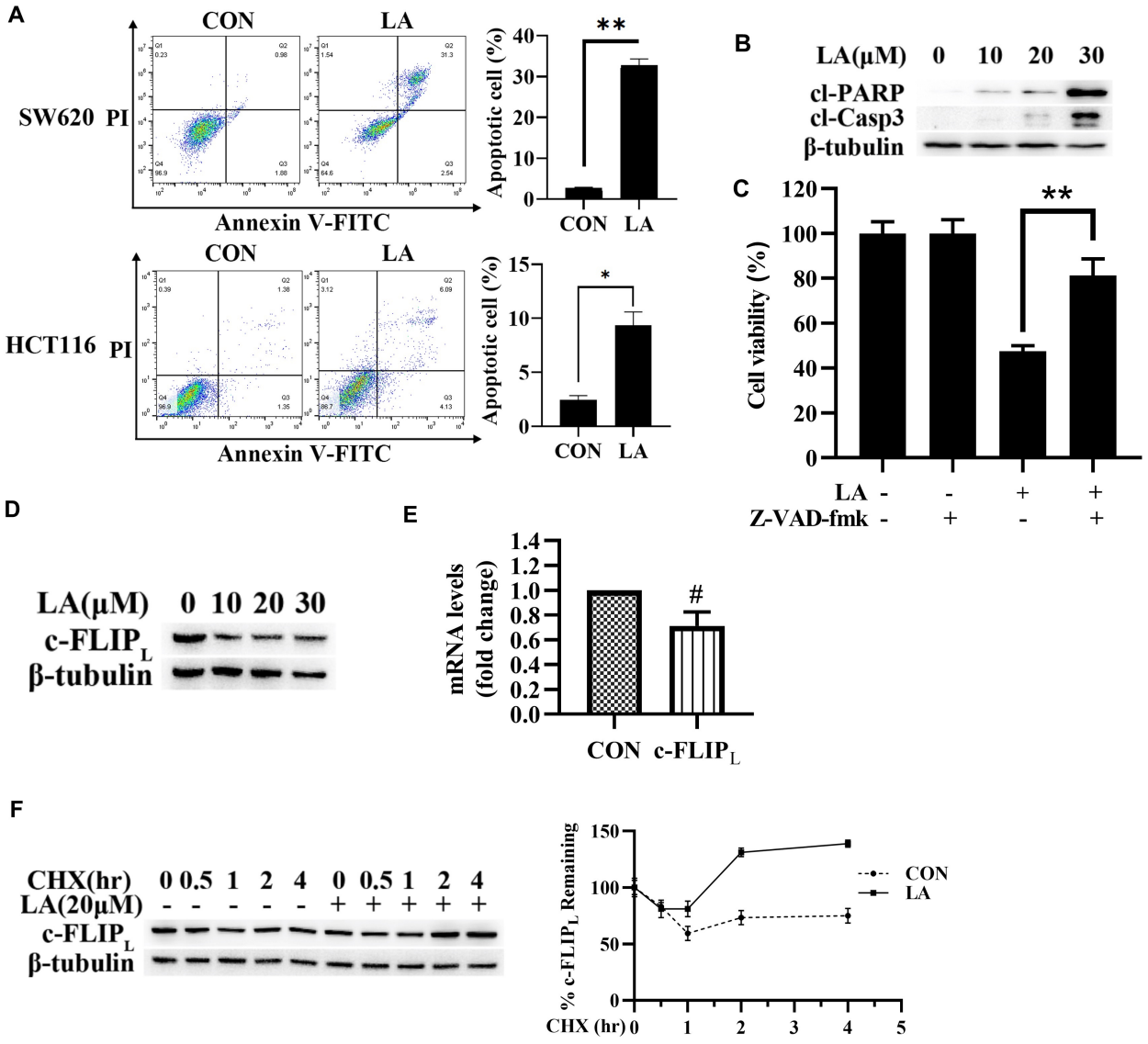

Fig. 2. LA triggered CRC cell apoptosis. (A) SW620 and HCT116 cell lines were cultured in 20 μM LA or DMSO, then flow cytometric assay was utilized to detect apoptotic cells at 48 h. (B) SW620 cell line grown with diverse thicknesses of LA. Next, the level of proteins was detected using immunoblotting at 48 h. (C) SW620 cell line was pretreated with 20 μM z-VAD-fmk. After 1 h, cells were cultured with 20 μM LA. Next, cell viabilities were measured using an MTT experiment at 48 h. (D) SW620 cells were grown with diverse thicknesses of LA; next, the level of c-FLIP$_L$ was measured by immunoblotting at 48 h. (E) SW620 cells were cultured with 20 μM LA. After that, all RNA was isolated, and c-FLIP$_L$ mRNA was detected by q-RT-PCR at 8 h. (F) SW620 cells were cultured with 20 μM LA or DMSO and, after 8 h, cultured with 200 μg/mL CHX for different times. After that, protein content was tested using immunoblotting. N = 3. *$p < 0.05$, **$p < 0.01$, #$p > 0.05$.

3.5 Hsp70 Maintained the Expression of c-FLIP$_L$ and Resisted LA-Induced Apoptosis

HSPs have been reported to inhibit apoptosis by assisting in the synthesis of apoptosis-related proteins [23]. Therefore, we detected the expression of Hsp70, Hsp90, HSPA4 (Hsp70 Family Member), and Hsp90α (Hsp90 Family Member) in CRC. Surprisingly, our results indicated that LA greatly enhanced the expression of Hsp70 rather than its mRNA level in SW620 cells (Fig. 5A and 5B). However, LA only marginally affects the expression of Hsp90, HSPA4, and Hsp90α. Furthermore, the cycloheximide chasing assay suggested that LA only marginally affected the degradation rate of Hsp70 and Hsp90 (Fig. 5C). This indicated that the enhancement of Hsp70 by LA was independent of transcription and degradation and could be involved in the mRNA translation.

Next, we found that CQ significantly inhibited Hsp70 expression (Fig. 5D), indicating that LA enhanced Hsp70

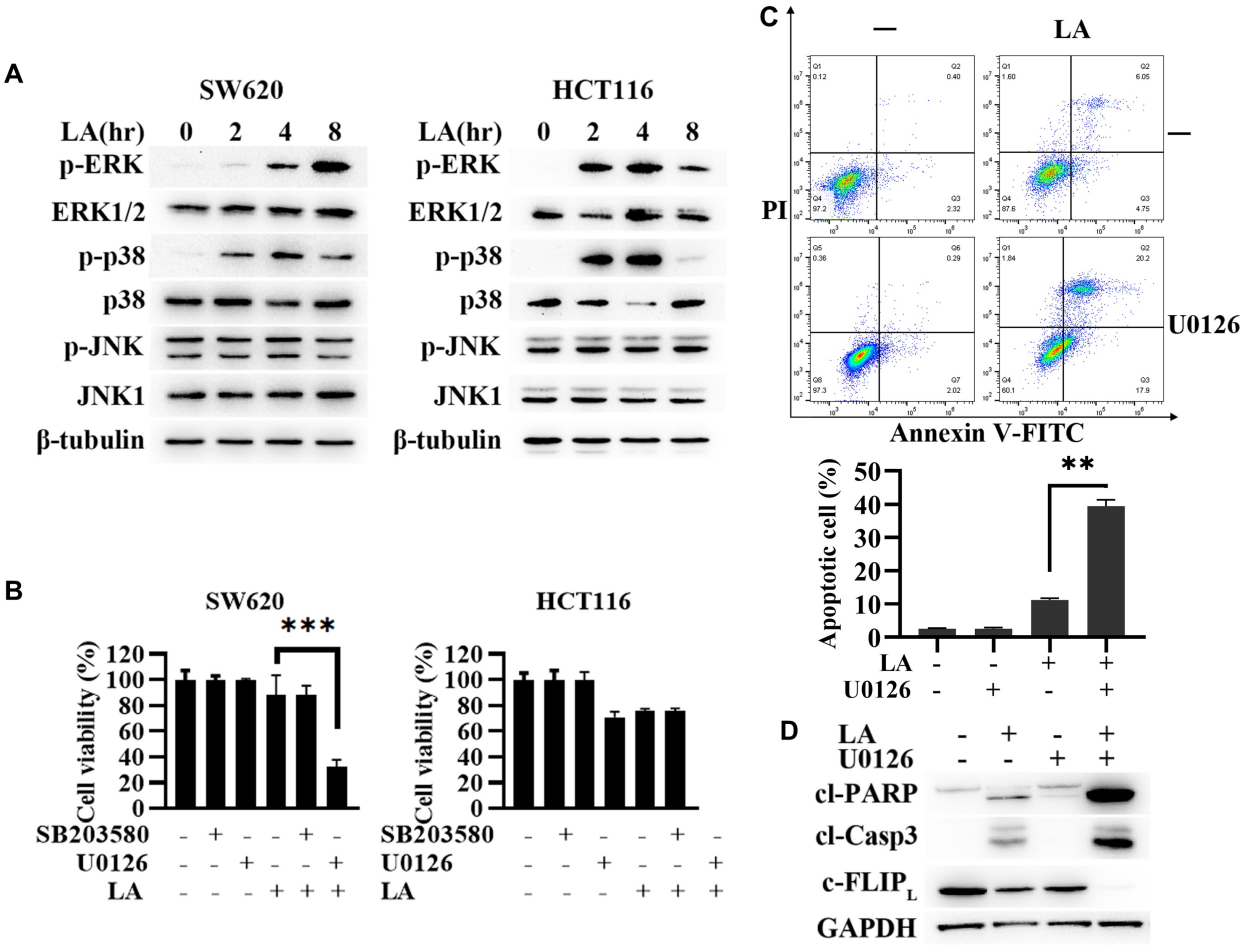

Fig. 3. ERK-mediated autophagic induction resisted LA-triggered anti-CRC activities. (A) SW620 and HCT116 cells were cultured with 20 μM LA; next, the level of proteins was measured by immunoblotting at different times. (B) SW620 and HCT116 cell line was pretreated with 20 μM U0126 and 20 μM SB203580. After 1 h, it was cultured with 20 μM LA for 48 h. After that, the viability of CRC cells was tested by MTT experiment. (C and D) SW620 cell line was cultured with 20 μM U0126. After 1 h, it was cultured with 20 μM LA; the apoptotic cell death was tested using flow cytometry (C), and the level of proteins was measured by immunoblotting (D) at 48 h. β-tubulin was measured as an input control. N = 3. $^{**}p < 0.01$, $^{***}p < 0.001$.

expression through autophagy activation. Then, the results of the MTT experiment and flow cytometry analysis indicated that MKT-077 (Hsp70 inhibitor) enhanced LA-triggered apoptosis (Fig. 5E and 5F). Moreover, MKT-077 enhanced cl-caspase-3 and cl-PARP and inhibited c-FLIP$_L$ (Fig. 5G). This indicated that Hsp70 resisted LA-triggered anticancer effects. Overall, autophagy activation mediated by ERK played a protective part in LA-triggered anti-CRC effects by enhancing the level of Hsp70 and sustaining the expression of c-FLIP$_L$ *in vitro*.

4. Discussion

As a tyrosinase inhibitor, LA has a wide range of pharmacological effects [10,25], and its anticancer effects have received more attention. The anticancer effects of LA were demonstrated *in vitro* and *in vivo* for a variety of tumors, including cervical cancer [15], prostate cancer [12,14], lung cancer [11], and breast cancer [13]. As a flavonoid, LA was affected by its strong hydrophobicity and the first-pass effect of the liver, resulting in its poor bioavailability [26]. However, it was reported that LA significantly increased the bioavailability by loading on liposome carriers or other nanocarriers [16,27–29]. In this study, LA was confirmed to have an anti-CRC effect at a dose that had no obvious toxicity to normal colonic epithelial cell line NCM460. In addition, LA had a better inhibitory effect on KRAS mutant cell lines (SW620 and HCT116) than KRAS wild-type HT29 cells. We speculated that this might be due to KRAS promoting tumor growth through activation of the PI3K/Akt pathway [30], while LA inhibited the PI3K/Akt

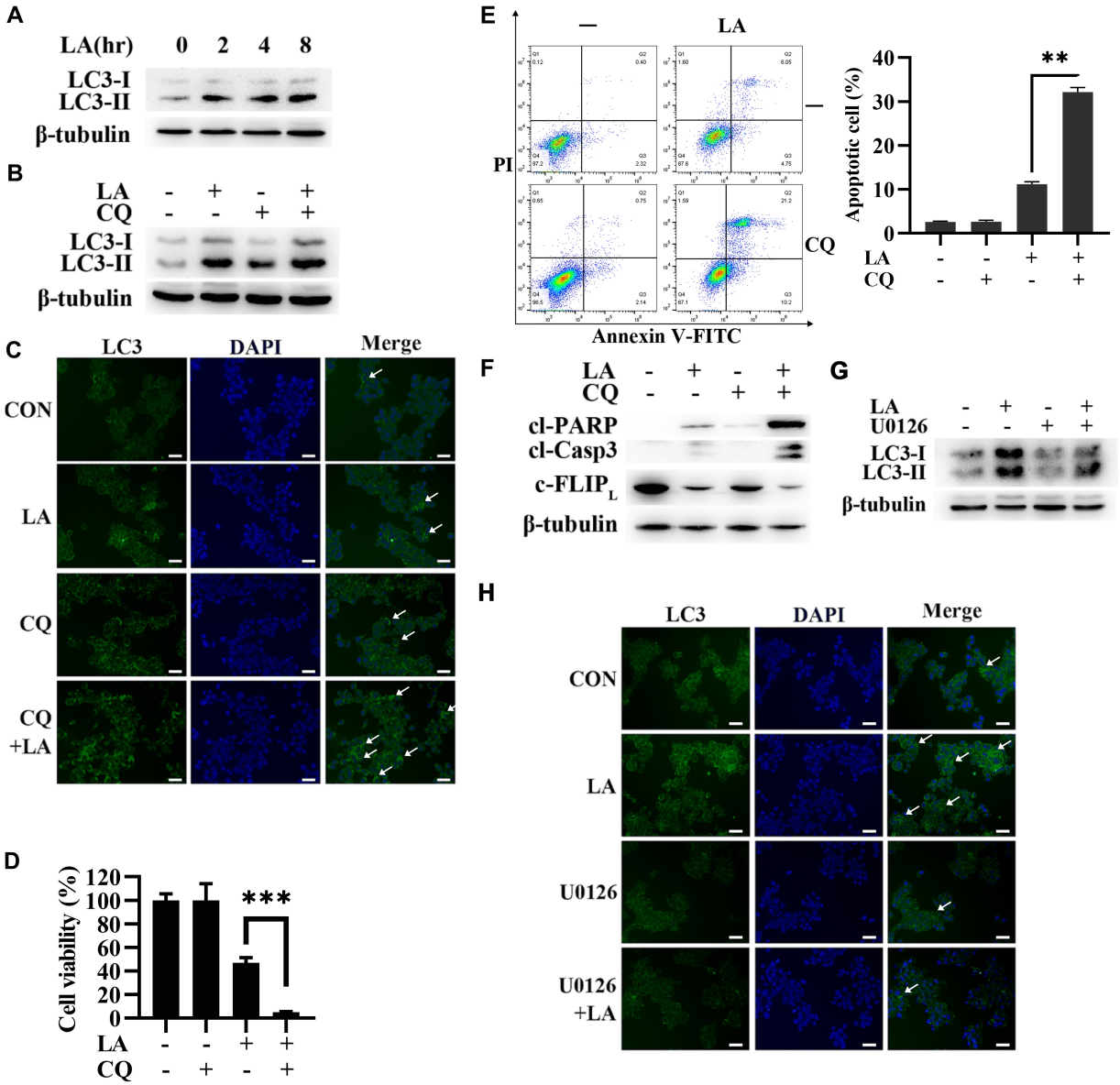

Fig. 4. Autophagy played a protective part for CRC cells in LA-triggered anticancer activities. (A) SW620 cells were cultured with 20 μM LA at different times; next, LC3 content was detected by immunoblotting. (B) SW620 cell line grown with 20 μM chloroquine (CQ). After 1 h, cells were cultured with 20 μM LA, then the level of LC3 was detected by immunoblotting at 8 h. (C) SW620 cell line grown with 20 μM CQ. After 1 h, cultured with 20 μM LA, then the level of LC3 was measured by immunofluorescence experiment at 8 h. Scale bar 100 μm. (D, E, and F) SW620 cell line grown with 20 μM CQ. After 1 h, cultured with 20 μM LA, then the viability of CRC cells was tested by MTT experiment (D), the apoptotic cell death was determined with flow cytometric assay (E), and the level of protein was determined by immunoblotting (F) at 48 h. (G and H) SW620 cell line was cultured with 10 μM U0126. After 1 h, it was cultured with 20 μM LA. After that, the level of LC3 was detected by immunoblotting (G) and immunofluorescence experiment (H) at 8 h. Scale bar 100 μm. β-tubulin and GAPDH were measured for input control. N = 3. $^{**}p < 0.01$, $^{***}p < 0.001$.

pathway [13,31,32]. Colony forming assay demonstrated that LA inhibited clonal proliferation of SW620 cells. Next, we elucidate the DNA synthesis of SW620 cell proliferation using EdU assays. Early studies showed that tumor growth and proliferation rapidly often lead to internal cell starvation without adequate nutrients [33]. Many herbal components, such as Anemarrhena asphodeloides, were reported to have a sensitizing anticancer with Serum starvation [34]. In the present research, LA was found to have a more significant anti-CRC effect with Serum starvation.

MAPK pathway was reported to be involved in LA-induced anti-multiple tumor effects [35–37]. In particular, activation of the MAPK/ERK plays a promoting role in the carcinogenic activity of human CRC [38]. Our re-

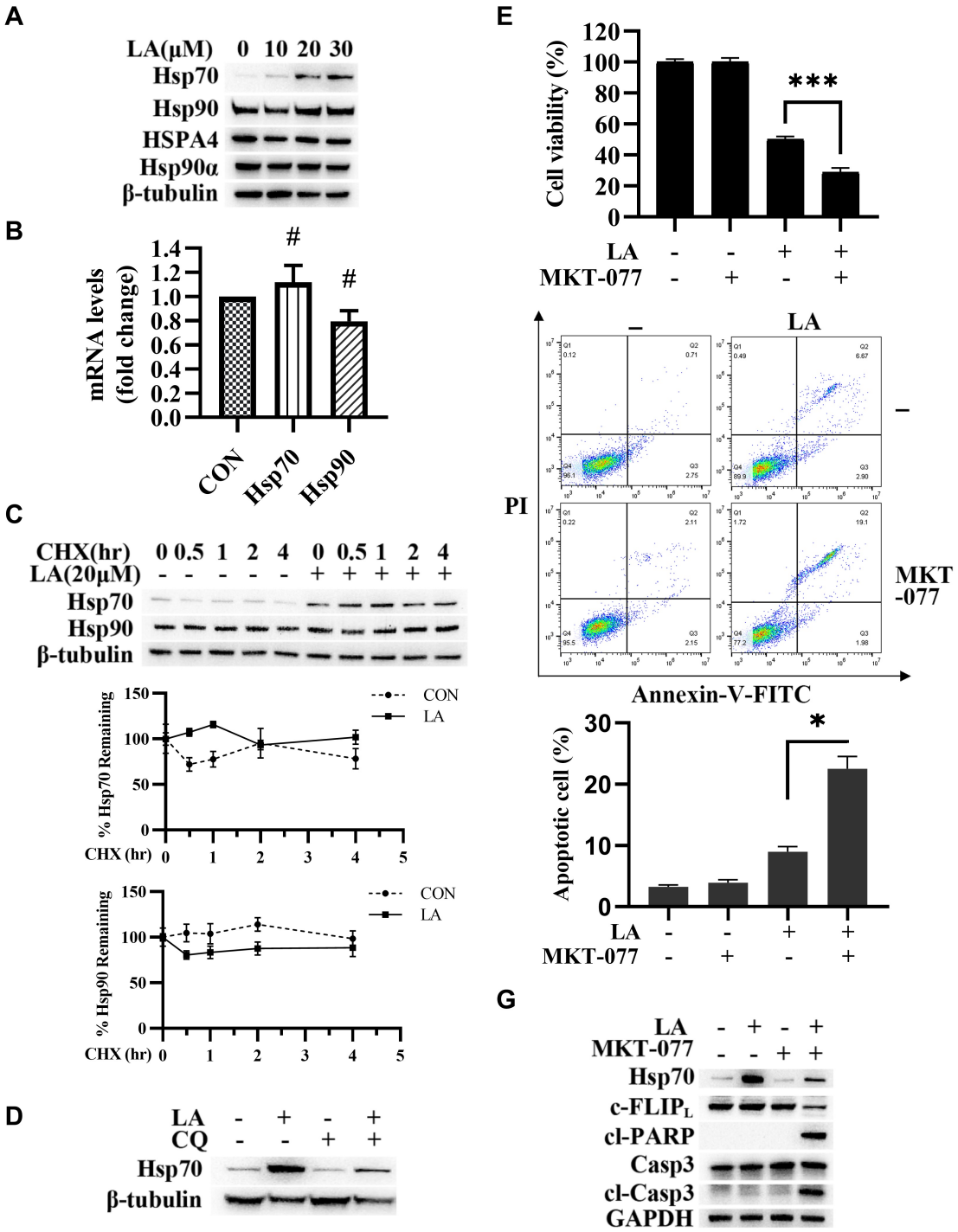

Fig. 5. Hsp70 expression maintained c-FLIP$_L$ expression and resisted LA-triggered apoptosis. (A) SW620 cell line was cultured with different thicknesses of LA. After 48 h, the level of protein was measured using immunoblotting. (B) SW620 cell line was cultured with 20 μM LA. After 8 h, all RNA in cells was isolated, and mRNA of Hsp70 and Hsp90 were detected by q-RT-PCR. (C) SW620 cell line grown with 20 μM LA or DMSO. After 8 h, it was cultured with 200 μg/mL CHX; next, the proteins were measured using immunoblotting at diverse times. (D) SW620 cell line grown with 20 μM CQ. After 1 h, it was cultured with 20 μM LA. After that, the level of Hsp70 was measured by immunoblotting at 8 h. (E, F, and G) SW620 cell line was cultured with 6 μM MKT-077 for 1 h, next, cultured with 20 μM LA for 48 h. After that, the viability of CRC cells was tested by MTT experiment (E), the apoptotic cell death was tested using flow cytometric analysis (F), and proteins were measured by immunoblotting (G). β-tubulin and GAPDH were measured for input control. N = 3. *$p < 0.05$, ***$p < 0.001$, #$p > 0.05$.

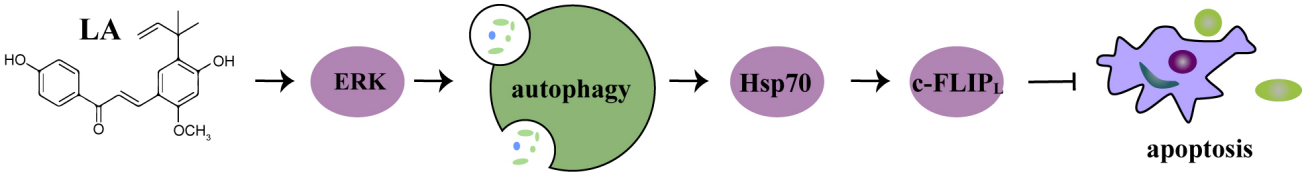

Fig. 6. LA-triggered anti-CRC activities. Hsp70 maintained c-FLIP$_L$ expression compromised LA-triggered anti-CRC activities through ERK-mediated autophagic induction.

sults showed that LA activated ERK and p38 in SW620 and HCT116 cells without significant effect on JNK. Subsequently, we found that inhibitors of ERK enhanced the LA-induced inhibition of SW620 cell viability, while inhibitors of p38 had no significant effect. This result suggested that it was ERK, not p38, involved in the anti-CRC pathway, although LA activated them in SW620 cells.

LA was found induced autophagy of CRC cells in our research. Autophagy is a catabolic process induced under stressful conditions. Lots of studies have confirmed that LA-induced autophagy plays different roles in different types of cancer cells [13–15,17,19]. Shen *et al.* [39] found that LA triggered autophagy in osteosarcoma cells, thus inhibiting cell proliferation and promoting apoptosis. It was reported that this might be because LA downregulated the autophagy protein p62 (which was described as a cancer-inducing factor [40,41]), thereby inhibiting tumor progression [42]. However, we found that the LA-induced autophagy was a cytoprotective autophagy and resisted the anticancer effect of LA in CRC. This conclusion was corroborated in studies of the anticancer effects of LA on cervical cancer [15] and lung cancer [9]. A recent study elucidated the mechanism by which some drugs or agents-induced autophagy could reduce the level of FOXO3a (a tumor suppressor protein) and thus downregulate the expression of the *Puma/Bbc3* (a pro-apoptotic gene) gene [43]. Then, the decreased *Puma/Bbc3* gene expression leads to increased drug resistance in tumor cells [43].

Our results showed that autophagy inhibited apoptosis by maintaining the continuous expression of the anti-apoptotic protein c-FLIP$_L$. Moreover, HSPs were reported to maintain c-FLIP$_L$ expression [20,21]. Consequently, we explored the role of HSPs in LA-triggered autophagic induction. The results discovered that LA enhanced Hsp70 by activating autophagy in CRC cells. Leu *et al.* [44] also described that autophagy enhanced Hsp70. However, Hsp70 also was reported to stabilize the lysosomal membrane, thereby promoting autophagy activation [45]. This might be because there was a large difference between physiological autophagy and stress-induced autophagy [42]. Therefore, we speculated that Hsp70 could stabilize physiological autophagy while drug-induced autophagy enhanced Hsp70. Then, we investigated the role of Hsp70 in LA-triggered anti-CRC activities. The results revealed that Hsp70 resisted LA-induced apoptosis by sustaining the expression level of c-FLIP$_L$ in CRC, just as in lung cancer [20]. This demonstrates that inhibition of Hsp70 was an effective strategy to enhance the anti-CRC effect of LA, and Hsp70 might be an effective target for anti-CRC.

Conclusively, LA induced cytoprotective autophagy through activation of ERK, and autophagy maintained c-FLIP$_L$ expression through upregulation of Hsp70, which in turn produced drug resistance (Fig. 6). However, there are still some limitations in this study. The results of this study should be verified by mRNA translation detection and the construction of drug-resistant cell lines. In addition, it is necessary to carry out *in vivo* experiments, including animal experiments, for the rigor of the experimental studies.

5. Conclusions

In conclusion, this study provided evidence that LA inhibited proliferation and induced apoptotic cell death of colorectal cancer, and Hsp70 sustained c-FLIP$_L$ expression to compromise LA-triggered anticancer effect through ERK-mediated autophagy induction *in vitro*. Therefore, LA combined with Hsp70 inhibitors might become a novel tactic for the therapy of CRC.

Availability of Data and Materials

The datasets created during this research are available from the corresponding author with rational requirement.

Author Contributions

TianL—conceptualization, data curation, methodology, project administration, validation, visualization, writing—original draft; TingL—methodology, project administration, validation, visualization, writing—review & editing; HZ—conceptualization, methodology, validation, visualization, writing—original draft; CL—data curation, methodology, validation, visualization, writing—original draft; ML—conceptualization, data curation, formal analysis, validation, visualization, writing—original draft; CW—conceptualization, methodology, data curation, validation, visualization, writing—original draft; YZ—data curation, validation, visualization, writing—original draft; LZ—conceptualization, data curation, validation, visualization, writing—review & editing; XL—data curation, validation, visualization, writing—review & editing; YL—data curation, validation, visualization, writing—review & editing; SS—data curation, validation, visualization, writing—review & editing; WC—data curation, validation,

visualization, writing—review & editing. All authors contributed to editorial changes in the manuscript. All authors read and approved the final manuscript. All authors have participated sufficiently in the work and agreed to be accountable for all aspects of the work.

Ethics Approval and Consent to Participate

Not applicable.

Acknowledgment

Not applicable.

Funding

This research was funded by National Natural Science Foundation of China (No. 81960156), High Level Reserve Talents in Health Science (H2018002), Medical edible flowers technology innovation team of universities in Yunnan province (2020YGC01), Kunming Medical University Applied basic Research Joint Project (202001AY070001-189, 202201AT070043), the Opening Project of Medical Imaging Key Laboratory of Sichuan Province (MIKLSP202004).

Conflict of Interest

The authors declare no conflict of interest.

References

[1] Siegel RL, Miller KD, Fuchs HE, Jemal A. Cancer Statistics, 2021. CA: A Cancer Journal for Clinicians. 2021; 71: 7–33.

[2] Siegel R, DeSantis C, Virgo K, Stein K, Mariotto A, Smith T, *et al*. Cancer treatment and survivorship statistics, 2012. CA: A Cancer Journal for Clinicians. 201; 62: 220–241.

[3] Brenner H, Bouvier AM, Foschi R, Hackl M, Larsen IK, Lemmens V, *et al*. Progress in colorectal cancer survival in Europe from the late 1980s to the early 21st century: the EUROCARE study. International Journal of Cancer. 2012; 131: 1649–1658.

[4] Sankaranarayanan R, Swaminathan R, Brenner H, Chen K, Chia KS, Chen JG, *et al*. Cancer survival in Africa, Asia, and Central America: a population-based study. The Lancet. Oncology. 2010; 11: 165–173.

[5] Jiang Y, Yuan H, Li Z, Ji X, Shen Q, Tuo J, *et al*. Global pattern and trends of colorectal cancer survival: a systematic review of population-based registration data. Cancer Biology & Medicine. 2021; 19: 175–186.

[6] He W, Wang Q, Srinivasan B, Xu J, Padilla MT, Li Z, *et al*. A JNK-mediated autophagy pathway that triggers c-IAP degradation and necroptosis for anticancer chemotherapy. Oncogene. 2014; 33: 3004–3013.

[7] Shi S, Wang Q, Xu J, Jang JH, Padilla MT, Nyunoya T, *et al*. Synergistic anticancer effect of cisplatin and Chal-24 combination through IAP and c-FLIPL degradation, Ripoptosome formation and autophagy-mediated apoptosis. Oncotarget. 2015; 6: 1640–1651.

[8] Xu J, Xu X, Shi S, Wang Q, Saxton B, He W, *et al*. Autophagy-Mediated Degradation of IAPs and c-FLIP(L) Potentiates Apoptosis Induced by Combination of TRAIL and Chal-24. Journal of Cellular Biochemistry. 2016; 117: 1136–1144.

[9] Luo W, Sun R, Chen X, Li J, Jiang J, He Y, *et al*. ERK Activation-Mediated Autophagy Induction Resists Licochalcone A-Induced Anticancer Activities in Lung Cancer Cells *in vitro*. Oncotargets and Therapy. 2021; 13: 13437–13450.

[10] Chen X, Liu Z, Meng R, Shi C, Guo N. Antioxidative and anticancer properties of Licochalcone A from licorice. Journal of Ethnopharmacology. 2017; 198: 331–337.

[11] Qiu C, Zhang T, Zhang W, Zhou L, Yu B, Wang W, *et al*. Licochalcone A Inhibits the Proliferation of Human Lung Cancer Cell Lines A549 and H460 by Inducing G2/M Cell Cycle Arrest and ER Stress. International Journal of Molecular Sciences. 2017; 18: 1761.

[12] Fu Y, Hsieh TC, Guo J, Kunicki J, Lee MY, Darzynkiewicz Z, *et al*. Licochalcone-a, a novel flavonoid isolated from licorice root (Glycyrrhiza glabra), causes G2 and late-G1 arrests in androgen-independent PC-3 prostate cancer cells. Biochemical and Biophysical Research Communications. 2004; 322: 263–270.

[13] Xue L, Zhang WJ, Fan QX, Wang LX. Licochalcone A inhibits PI3K/Akt/mTOR signaling pathway activation and promotes autophagy in breast cancer cells. Oncology Letters. 2018; 15: 1869–1873.

[14] Yo YT, Shieh GS, Hsu KF, Wu CL, Shiau AL. Licorice and licochalcone-A induce autophagy in LNCaP prostate cancer cells by suppression of Bcl-2 expression and the mTOR pathway. Journal of Agricultural and Food Chemistry. 2009; 57: 8266–8273.

[15] Tsai JP, Lee CH, Ying TH, Lin CL, Lin CL, Hsueh JT, *et al*. Licochalcone A induces autophagy through PI3K/Akt/mTOR inactivation and autophagy suppression enhances Licochalcone A-induced apoptosis of human cervical cancer cells. Oncotarget, 2015; 6: 28851–28866.

[16] Liu J, Zhu Z, Yang Y, Adu-Frimpong M, Chen L, Ji H, *et al*. Preparation, characterization, pharmacokinetics, and antirenal injury activity studies of Licochalcone A-loaded liposomes. Journal of Food Biochemistry. 2022; 46: e14007.

[17] Tang ZH, Chen X, Wang ZY, Chai K, Wang YF, Xu XH, *et al*. Induction of C/EBP homologous protein-mediated apoptosis and autophagy by licochalcone A in non-small cell lung cancer cells. Scientific Reports. 2016; 6: 26241.

[18] Hu L, Wang Y, Chen Z, Fu L, Wang S, Zhang X, *et al*. Hsp90 Inhibitor SNX-2112 Enhances TRAIL-Induced Apoptosis of Human Cervical Cancer Cells via the ROS-Mediated JNK-p53-Autophagy-DR5 Pathway. Oxidative Medicine and Cellular Longevity. 2019; 2019: 9675450.

[19] Chen G, Ma Y, Jiang Z, Feng Y, Han Y, Tang Y, *et al*. Lico A Causes ER Stress and Apoptosis via Up-Regulating miR-144-3p in Human Lung Cancer Cell Line H292. Frontiers in Pharmacology. 201; 9: 837.

[20] Zhuang H, Jiang W, Zhang X, Qiu F, Gan Z, Cheng W, *et al*. Suppression of HSP70 expression sensitizes NSCLC cell lines to TRAIL-induced apoptosis by upregulating DR4 and DR5 and downregulating c-FLIP-L expressions. Journal of Molecular Medicine. 2013; 91: 219–235.

[21] Wang Q, Sun W, Hao X, Li T, Su L, Liu X. Down-regulation of cellular FLICE-inhibitory protein (Long Form) contributes to apoptosis induced by Hsp90 inhibition in human lung cancer cells. Cancer Cell International. 2012; 12: 54.

[22] Li J, Sun L, Xu C, Yu F, Zhou H, Zhao Y, *et al*. Structure insights into mechanisms of ATP hydrolysis and the activation of human heat-shock protein 90. Acta Biochimica et Biophysica Sinica. 2012; 44: 300–306.

[23] Zhao D, Xu YM, Cao LQ, Yu F, Zhou H, Qin W, *et al*. Complex Crystal Structure Determination and *in vitro* Anti-non-small Cell Lung Cancer Activity of Hsp90N Inhibitor SNX-2112. Frontiers in Cell and Developmental Biology. 2021; 9: 650106.

[24] Shirley S, Micheau O. Targeting c-FLIP in cancer. Cancer Letters. 2013; 332: 141–150.

[25] Kim YH, Shin EK, Kim DH, Lee HH, Park JH, Kim JK. Antiangiogenic effect of licochalcone A. Biochemical Pharmacology. 2010; 80: 1152–1159.

[26] Weng Q, Chen L, Ye L, Lu X, Yu Z, Wen C, *et al*. Determination of licochalcone a in rat plasma by UPLC–MS/MS and its pharmacokinetics. Acta Chromatographica. 2019; 31: 262–265.
[27] Zhu Z, Liu J, Yang Y, Adu-Frimpong M, Ji H, Toreniyazov E, *et al*. SMEDDS for improved oral bioavailability and anti-hyperuricemic activity of licochalcone A. Journal of Microencapsulation. 2021; 38: 459–471.
[28] Sun Y, Wang L, Meng D, Che X. A green and facile preparation approach, licochalcone a capped on hollow gold nanoparticles, for improving the solubility and dissolution of anticancer natural product. Oncotarget. 2017; 8: 105673–105681.
[29] Silva LM, Marconato DG, Nascimento da Silva MP, Barbosa Raposo NR, Faria Silva Facchini G, Macedo GC, *et al*. Licochalcone A-loaded solid lipid nanoparticles improve antischistosomal activity *in vitro* and *in vivo*. Nanomedicine. 2021; 16: 1641–1655.
[30] Castellano E, Downward J. RAS Interaction with PI3K: More Than Just Another Effector Pathway. Genes & Cancer. 2011; 2: 261–274.
[31] Huang HC, Tsai LL, Tsai JP, Hsieh SC, Yang SF, Hsueh JT, *et al*. Licochalcone A inhibits the migration and invasion of human lung cancer cells via inactivation of the Akt signaling pathway with downregulation of MMP-1/-3 expression. Tumour Biology. 2014; 35: 12139–12149.
[32] Wu J, Zhang X, Wang Y, Sun Q, Chen M, Liu S, *et al*. Licochalcone A suppresses hexokinase 2-mediated tumor glycolysis in gastric cancer via downregulation of the Akt signaling pathway. Oncology Reports. 2018; 39: 1181–1190.
[33] Hanahan D, Weinberg R. Hallmarks of Cancer: the next Generation. Cell. 2011; 144: 646–674.
[34] Ji KY, Kim KM, Kim YH, Shim KS, Lee JY, Kim T, *et al*. Serum Starvation Sensitizes Anticancer Effect of Anemarrhena asphodeloides via p38/JNK-Induced Cell Cycle Arrest and Apoptosis in Colorectal Cancer Cells. The American Journal of Chinese Medicine. 2021; 49: 1001–1016.
[35] Hao W, Yuan X, Yu L, Gao C, Sun X, Wang D, *et al*. Licochalcone A-induced human gastric cancer BGC-823 cells apoptosis by regulating ROS-mediated MAPKs and PI3K/AKT signaling pathways. Scientific Reports. 2015; 5: 10336.
[36] Lin RC, Yang SF, Chiou HL, Hsieh SC, Wen SH, Lu KH, *et al*. Licochalcone A-Induced Apoptosis Through the Activation of p38MAPK Pathway Mediated Mitochondrial Pathways of Apoptosis in Human Osteosarcoma Cells *In Vitro* and *In Vivo*. Cells. 2019; 8: 1441.
[37] Park MR, Kim SG, Cho IA, Oh D, Kang KR, Lee SY, *et al*. Licochalcone-A induces intrinsic and extrinsic apoptosis via ERK1/2 and p38 phosphorylation-mediated TRAIL expression in head and neck squamous carcinoma FaDu cells. Food and Chemical Toxicology. 2015; 77: 34–43.
[38] Fang JY, Richardson BC. The MAPK signalling pathways and colorectal cancer. The Lancet Oncology. 2005; 6: 322–327.
[39] Shen TS, Hsu YK, Huang YF, Chen HY, Hsieh CP, Chen CL. Licochalcone A Suppresses the Proliferation of Osteosarcoma Cells through Autophagy and ATM-Chk2 Activation. Molecules. 2019; 24: 2435.
[40] Umemura A, He F, Taniguchi K, Nakagawa H, Yamachika S, Font-Burgada J, *et al*. P62, Upregulated during Preneoplasia, Induces Hepatocellular Carcinogenesis by Maintaining Survival of Stressed HCC-Initiating Cells. Cancer Cell. 2016; 29: 935–948.
[41] Yang W, Wei J, Lv L, Xie J, Li A, Zheng Z, *et al*. p62 Promotes Malignancy of Hepatocellular Carcinoma by Regulating the Secretion of Exosomes and the Localization of β-Catenin. Frontiers in Bioscience-Landmark. 2022; 27: 89.
[42] Amaravadi RK, Kimmelman AC, Debnath J. Targeting Autophagy in Cancer: Recent Advances and Future Directions. Cancer Discovery. 2019; 9: 1167–1181.
[43] Fitzwalter BE, Thorburn A. FOXO3 links autophagy to apoptosis. Autophagy. 2018; 14: 1467–1468.
[44] Leu JI, Pimkina J, Pandey P, Murphy ME, George DL. HSP70 Inhibition by the Small-Molecule 2-Phenylethynesulfonamide Impairs Protein Clearance Pathways in Tumor Cells. Molecular Cancer Research. 2011; 9: 936–947.
[45] Daugaard M, Kirkegaard-Sørensen T, Ostenfeld MS, Aaboe M, Høyer-Hansen M, Orntoft TF, *et al*. Lens epithelium-derived growth factor is an Hsp70-2 regulated guardian of lysosomal stability in human cancer. Cancer Research. 2007; 67: 2559–2567.